brief communication

# Protein dynamics and 1/f noise

T. Gregory Dewey and James G. Bann
Department of Chemistry, University of Denver, Denver, Colorado 80208 USA

ABSTRACT It has long been recognized that protein dynamical processes occur over a wide temporal range. However, the functionality of this spectrum of events remains unclear. In this work, a generalized noise function analysis is applied to a collection of diverse protein dynamical systems. It is shown that a power law model with an oscillatory component can adequately describe the time course of a variety of processes. These results suggest that under the appropriate conditions, proteins are in a metastable state. A microscopic, chemical kinetic model based on a Poisson distribution of activation energies is presented. From this model specific functional forms for the parameters of the generalized noise model can be derived. Additionally, a model is presented to describe kinetic hole burning effects observed at low temperatures. Scaling laws are derived for these models that provide a connection with the generalized noise analysis.

## INTRODUCTION

The diversity of phenomenon which exhibit $1/f$ noise has intrigued physical scientists for a number of years (for reviews see references 1–3). The dynamics of such wide-ranging systems as the human heart, river discharges, resistors and cellular membranes all show low frequency power spectra that, obey a $1/f^{\beta}$ law, where $f$ is frequency and $\beta$ is a constant. Recent work on this problem has focused on the self-organized criticality of systems of minimal stability (4, 5). Unlike the criticality observed in phase transitions, this dynamical effect is insensitive to the "tuning" of the parameters of the system and achieves its scaling properties even when starting far from equilibrium. A number of specific models have been developed that successfully explain this behavior (cf. reference 6). In addition to predicting a $1/f^{\beta}$ power law, these models give oscillatory components that have been observed in some systems (6).

In this work we examine a number of unrelated protein systems for behavior consistent with generalized noise models. These examples, taken from the literature, were chosen both because measurements were made over several orders of magnitude in time and because they demonstrate nonexponential kinetics. Previously, a number of different models have been used to describe this nonexponential behavior (for a review see reference 7). These models fall into three general categories: structural disorder, dynamical disorder, and fractal. Whereas each model can adequately fit the data for a given application, no single one of these models has shown general applicability. In this work it is demonstrated that the generalized noise model can fit a diverse range of data.

## ANALYSIS OF EXPERIMENTAL DATA

Processes exhibiting $1/f^{\beta}$ behavior can be established using a renormalization of a dynamical variable, $\phi(t)$, such that (6, 8):

$$\phi(t) = (p/N)\phi(t/N). \tag{1}$$

A general solution of this functional equation is:

$$\phi(t) = t^{-\mu-1}A(t), \tag{2}$$

where $\mu = \ln(1/p)/\ln N$ and $A(t)$ is an oscillatory function periodic in $\log t$:

$$A(t) = \sum_{n=0}^{\infty} A_n e^{i2n\pi \ln t/\ln N}. \tag{3}$$

Power laws with an oscillatory component have arisen in a variety of contexts. Our goal is to establish whether Eq. 2 provides a phenomenological description of protein dynamics. Previously, power law models derived from reptation theory have been used to describe ion channel gating (9, 10). These models do not contain an oscillatory component and complex, multistep mechanisms must be evoked to adequately fit experimental data. In this work ion channel gating data as well as data from a number of other nonexponential processes were chosen from the literature and were fit to the function:

$$\phi(t) = (A_2 + A_3 \cos(A_4 \ln t))/t^{A_1}. \tag{4}$$

where $A_i$ represent adjustable parameters that are determined by the Marquardt nonlinear least squares fitting routine. Using Eq. 4, good statistical fits were obtained for the following rate processes: tritium exchange in the membrane-bound protein, rhodopsin (11), and in the soluble protein, lysozyme (12), CO photodissociation of myoglobin (13), and gating kinetics of ion channels (14). Table 1 shows the fitted parameters for these cases. Figs. 1 and 2 show specific examples of the fit of Eq. 4 to the experimental data. These examples were ones in which the oscillatory component was particularly prominent. As can be seen, the main features of the data are fit quite well. It should be emphasized that Eq. 4 is a "minimal" representation of Eq. 3 because higher order oscil-

Address correspondence to T. Gregory Dewey.


0006-3495/92/08/594/05 $2.00

TABLE 1 **Fitted parameters for generalized noise model**

| Dynamical process (reference) | Critical exponent $A_1(\alpha)$* | Periodicity $A_4$ | Amplitude ratio $A_3/A_2$ |
|---|---|---|---|
| Tritium exchange in rhodopsin (11) | 0.53 (0.53) | 1.08 | 0.33 |
| Tritium exchange in lysozyme (12) | 0.25 (0.25) | 0.07 | −1.01 |
| Endplate channel open intervals (14)‡ | 1.29 (0.29) | 1.39 | −0.71 |
| Endplate channel closed intervals (14) | 1.0 (0.0) | 0.90 | 0.84 |
| CO photodissociation from myoglobin (13)§ | | | |
| (100°K) | 0.038 (.92) | 1.01 | −0.014 |
| (120°K) | 0.042 (.91) | 1.03 | −0.014 |

* For all data except the channel data, $A_1 = \alpha$. The channel data is given in terms of the probability density per unit time. As discussed in the text this case will give $A_1 = \alpha - 1$. All data is at room temperature unless otherwise specified. ‡This data is represented in Fig. 1. Other data from reference 13 require higher order harmonics for adequate fits. §All data from (reference 14) were accurately fit and are shown in Fig. 2.

lations were not included. Obviously, the fits could be further refined by including higher harmonics.

## A CHEMICAL KINETIC MODEL

From the above results, it is seen that Eq. 4 provides an adequate fitting function for a number of different protein dynamical processes. Whereas this establishes a good phenomenological description of these processes, ultimately one requires a microscopic model of the dynamics. Presently, we demonstrate that relatively simple kinetic models can generate rate expressions analogous to Eq. 4. We consider an adaptation of the activation energy dispersion model used by Bendler and Shlesinger to describe defect diffusion in polymers (15). In this model, thermally activated jump kinetics must be averaged over a dispersion in the activation energy. In this case, the distribution of activation energies may result from the existence of conformational substates as discussed by Frauenfelder and co-workers (16).

The phenomenological rate constant, $k_0$, is assumed to be:

$$k_0 = A \exp\{-G_0^+/kT\}, \tag{5}$$

where $G_0^+$ is the free energy of the barrier and $A$ is the frequency factor. The dispersion in the barrier is given by:

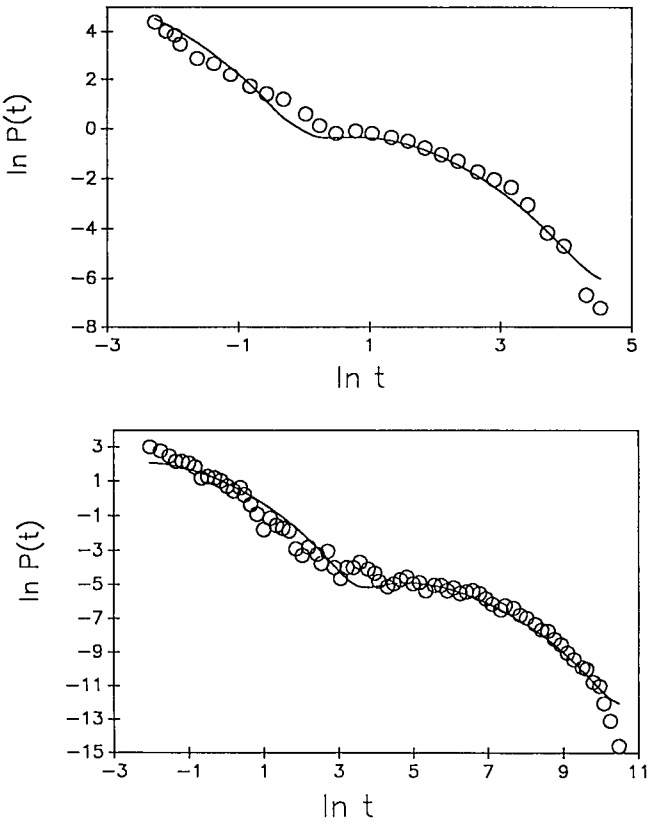


FIGURE 1 Distributions of open (*top*) and shut (*bottom*) interval durations, $P(t)$, versus time for endplate channels (see reference 14). Solid lines are curves obtained from a nonlinear least squares fit to Eq. 4 (four adjustable parameters). Further refinement in the fit can be made by including higher order harmonics. Previously these curves required a sum of four (*top*) and six (*bottom*) exponentials to fit the data (14).

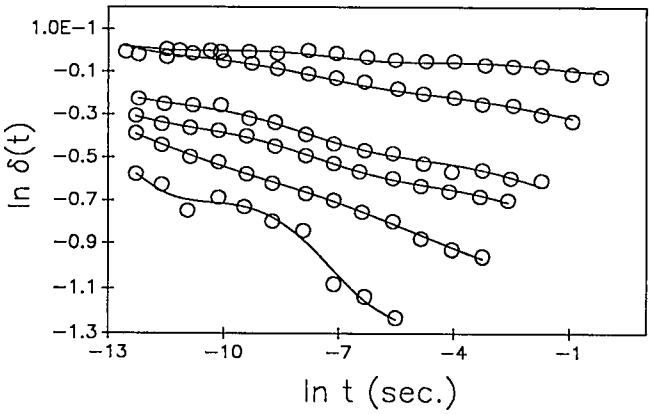


FIGURE 2 Plot of the parameter $\delta(t)$ versus time for the photodissociation of CO from myoglobin (see reference 13). The parameter, $\delta(t)$, is proportional to the extent of the reaction. Solid lines are curves obtained from a nonlinear least squares fit to Eq. 4 (four adjustable parameters). Each curve represents data for a different temperature. Temperature from top to bottom are 60, 80, 100, 120, 140, and 160°K.

$$G^+ = H^+ - TS^+ = H_0^+ + \delta H^+ - T(S_0^+ + \delta S^+), \quad (6)$$

where $\delta H^+$ and $\delta S^+$ are the variations in the enthalpy and entropy, respectively. As in the previous model (15), we will assume for simplicity that entropy-enthalpy compensation exists. Thus, $\sigma\delta H^+ = \delta S^+$, where $\sigma^{-1}$ has units of temperature. The rate constant, $k$, including the dispersive term, is given by:

$$k = k_0 \exp\{-\delta H^+(1 - \sigma T)/RT\}. \quad (7)$$

For a unimolecular process the decay of reactant concentration, $C(t)$, is now given by:

$$dC/dt = kC. \quad (8)$$

This expression is integrated and then averaged over all possible values for the rate constant, giving:

$$\langle C(t)\rangle = C_0 \int \rho(k)e^{-kt}\, dk, \quad (9)$$

where $C_0$ is the initial concentration and $\rho(k)$ is the probability density of a state associated with the rate constant, $k$. Our goal now is to establish a correspondence with a renormalization group analogue, providing a functional equation similar to Eq. 1. It proves convenient to use the temporal Laplace transform of Eq. 9, giving:

$$\tilde{C}(\epsilon) = C_0 \int dk\rho(k) \Big/ \{\epsilon + k\}. \quad (10)$$

Scaling of $\epsilon$ by $\epsilon/b$ gives:

$$\tilde{C}(\epsilon/b) = C_e \int dk'\rho(k'/b) \Big/ \{\epsilon + k'\}, \quad (11)$$

where $k' = kb$. If the dispersion in activation energy is assumed to follow a Poisson distribution law, as in the polymer case (15), then:

$$\rho(k) = q \exp\{-\delta H^+ q\} = q(k/k_0)^{qRT/(1-\sigma T)}, \quad (12)$$

where $q$ is the probability density per unit energy. Using Eq. 12 in 11 then gives the scaling law:

$$\tilde{C}(\epsilon) = b^{-\alpha}\tilde{C}(\epsilon/b), \quad (13)$$

where $\alpha = qRT/(1 - \sigma T)$. This functional equation is solved as described previously (8). The general solution will have a singular component which is responsible for the oscillatory behavior. It is given by:

$$\tilde{C}(\epsilon) = \epsilon^H K(\epsilon), \quad (14)$$

with $H = \ln(b^{\alpha-1})/\ln b = \alpha - 1$ and $K(\epsilon)$ is a function periodic in $\ln \epsilon$ with period $\ln(b^{-1})$.

To obtain the functional form (Eq. 4) used to analyze protein dynamical processes, Eq. 14 is Laplace inverted. When the observable is proportional to the extent of the reaction, the fitted parameters, $A_1$ and $A_4$ in Eq. 4 are $A_1 = \alpha$ and $A_4 = 2\pi \ln(b^{-1})$. There are often experimental cases, such as ion channel gating, in which the experimental data is represented as a probability per unit time, $P(t)$. In these instances, the analogue of Eq. 9 becomes:

$$P(t) = \int \rho(k)ke^{-kt}\, dk, \quad (15)$$

and the corresponding scaling law is:

$$\tilde{P}(\epsilon) = b^{1-\alpha}\tilde{P}(\epsilon/b). \quad (16)$$

An equation of the form of Eq. 4 is again recovered, except now $A_1 = \alpha - 1$. This different expression is used in the analysis of the ion gating data as shown in Table 1.

## A MODEL FOR KINETIC HOLE BURNING

Frauenfelder and co-workers have extensively investigated kinetic hole burning of spectral bands after photodissociation of CO from myoglobin (for a recent review see reference 17). Initially, results at low temperature were interpreted as a relaxation phenomenon (13). As a consequence of theoretical (18, 19) and experimental (20, 21) studies, it became apparent that such a model is inappropriate for treating low temperature data on the shift of spectral bands (<170°K). Under these conditions the absorbance spectra of myoglobin shows inhomogenous broadening and kinetic hole-burning effects dominate.

In this section, a generalized noise analysis is applied to kinetic data for inhomogenous broadened systems. The approach of Steinbach et al. (22) is adapted for these purposes. When monitoring the kinetics of inhomogenous systems, the absorbance spectra, $A$, is a complicated function of the frequency of the absorbed light, $\nu$, and time, $t$. This function will be given by:

$$A(\nu, t) = K \int d\nu' D(\nu', \nu_p)S(\nu, \nu', t), \quad (17)$$

where $K$ is a constant and $S$ is a homogeneous Lorenzian lineshape. There is a superposition of Lorenzians which have a distribution given by the function, $D$. The Lorenzian, $S$, is:

$$S(\nu, \nu', t) = N_{\nu'}[(\nu - \nu')^2 + \Gamma_h^2/4]^{-1}, \quad (18)$$

where $\Gamma_h$ is the homogeneous contribution to the lineshape and $N_\nu$ is the amplitude and is proportional to the number of molecules with spectra centered on the Lorenzian. The time dependence is directly incorporated by the exponential decrease in $N_\nu$ and gives:

$$S(\nu, \nu', t) = Ne^{-k_{\nu'}t}[(\nu - \nu')^2 + \Gamma_h^2/4]^{-1}, \quad (19)$$

where $k_{\nu'}$ is the rate constant associated with molecules at this spectral position. The inhomogenous spectral distribution, $D(\nu', \nu_p)$, was taken as a Gaussian in the previous application (22). In our case, we choose a Poisson

distribution as in Eq. 12. This choice will provide a scaling law in accordance with Eq. 1. The Poisson distribution gives:

$$D(\nu', \nu_p) = (1/\Gamma_i) \exp\{-(\nu' - \nu_p)/\Gamma_i\}, \quad (20)$$

where $\nu_p$ is the peak frequency and the distribution has a variance of $\Gamma_i$. The Steinbach model asserts that there is a linear mapping between the kinetic barrier distribution and the inhomogeneous distribution. The barrier height, $H$, is then related to the spectral position by:

$$H(\nu') = H_p + (\Gamma_h/\Gamma_i)(\nu' - \nu_p). \quad (21)$$

At the temperatures under consideration quantum mechanical tunneling is not a factor and the rate constant, $k_{\nu'}$ is then given by the standard Eyring form:

$$k_{\nu'} = (C/T)e^{-H(\nu')/RT}, \quad (22)$$

where $C$ is a constant.

Combining these results, the absorbance is given by:

$$A(\nu, t) = K \int d\nu' \frac{Ne^{-k_{\nu'}t}e^{-(\nu'-\nu_p)/\Gamma_i}}{\Gamma_i\{(\nu - \nu')^2 + \Gamma_h^2/4\}}. \quad (23)$$

It proves more convenient to transform the variable from $\nu'$ to $k_{\nu'}$. This transformation gives:

$$A(k_{\nu'}, t) = -(RTKN/\Gamma_h k_p^{\alpha}) \times \int dk_{\nu'} \frac{k_{\nu'}^{1-\alpha}e^{-k_{\nu'}t}}{((RT\Gamma_i/\Gamma_h)\ln(k_{\nu'}/k_\nu))^2 + \Gamma_h^2/4}, \quad (24)$$

where the parameter, $\alpha = RT/\Gamma_h$. As in the previous section, the temporal Laplace transform is taken and is designated $\tilde{A}(k_{\nu'}\epsilon)$. Using the same approach as in Eqs. 10 and 11, it is readily shown that:

$$\tilde{A}(k_{\nu'}\epsilon) = b^{1-\alpha}\tilde{A}(k_{\nu'}\epsilon/b). \quad (25)$$

Upon Laplace transformation Eq. 25, like Eq. 16, will have a time dependence, $A(k_{\nu'}t) \propto t^{1-\alpha}$.

The measured quantity in the hole-burning experiment on myoglobin (13) is the shift of peak position (band III at 760 nm), $\delta(t)$, as a function of time. This shift is a consequence of the inhomogeneous broadening of the spectral line and of the correlation of spectral position with kinetic barrier height. Our goal is to establish the temporal scaling behavior of $\delta(t)$. To achieve this, the scaling properties of the short time behavior of the system is established. The extension of these properties to longer times will be tested by the ability to fit the data. In the previous notation, the change in peak position from time $t$ to $t'$ is given by:

$$\delta(t') = \nu_{max}(t = t') - \nu_{max}(t = 0), \quad (26)$$

where $\nu_{max}$ is the position of the spectral peak. To relate this parameter to the expressions for the absorbance, $A(\nu, t)$, a Taylor series expansion about the peak maxima is performed. We will consider two spectral regions; $\nu_1$, the maxima at $t = 0$ and $\nu_2$, the maxima at $t = t'$. If $t$ is short, then $\delta(t)$ will be small and the absorbance properties at these two frequencies can be related to each other by the early terms of the series expansion. First, we expand $A(\nu_2, t = 0)$, about the maxima at $t = 0$, $\nu_1$:

$$A(\nu_2, t = 0) = A(\nu_1, t = 0) + (1/2)(\partial^2 A/\partial t^2)_{\nu 1}(\nu_2 - \nu_1)^2. \quad (27)$$

The term linear in frequency will be zero as a consequence of expanding about the maxima. The quadratic term is retained to describe the behavior in the region of the maxima. Next, an expansion is taken for $A(\nu_1, t = t')$ about $\nu_2$, the maxima at $t = t'$:

$$A(\nu_1, t = t') = A(\nu_2, t = t') + (1/2)(\partial^2 A/\partial t^2)_{\nu 2}(\nu_1 - \nu_2)^2. \quad (28)$$

Note that $\delta(t) = \nu_2 - \nu_1$. Also, $\Delta A(\nu) = A(\nu, t = t') - A(\nu, t = 0)$ and $\Delta A$ follows the same scaling law as $A(\nu, t)$. Adding Eqs. 27 and 28 and rearranging gives:

$$\delta(t) = [(\Delta A(\nu_1) - \Delta A(\nu_2))/((\partial^2/\partial\nu^2)_{\nu 1} + (\partial^2/\partial\nu^2)_{\nu 2})]^{1/2}. \quad (29)$$

For small displacements of frequency, the curvature of the peak changes very little and the second derivatives in Eq. 29 can be treated as independent of time. From Eq. 25, the scaling behavior for the Laplace transform of $\delta(t)$ is:

$$\tilde{\delta}(\epsilon) = b^{(1-\alpha)/2}\tilde{\delta}(\epsilon/b). \quad (30)$$

The fitting parameter, $A_1$, then becomes $(1 - \alpha)/2$.

Fig. 2 shows the fit of Eq. 4 to the photodissociation of myoglobin at a number of different temperatures. As can be seen the change in peak position, $\delta(t)$, versus time is readily fit over the entire temperature range. The logarithmic oscillations are apparent from the plot. From the fitted parameter, $A_1$, the value for $\Gamma_i$ can be determined at each temperature. Not surprisingly, this parameter shows a temperature dependence, starting with a value of 44 $cm^{-1}$ at 60°K and ending with a value of 136 $cm^{-1}$ at 160°K. It is interesting to compare these values with those obtained previously from a model that assumes a Gaussian distribution for the inhomogeneous broadening (22). In this case, bandwidths ranged from ~140 to 175 $cm^{-1}$ over the temperature range under consideration (parameter $(M_2)^{1/2}$ in the notation of the reference 22). Because of the difference in the two models, one does not expect agreement in this parameter. These results do show that physically realistic values are being obtained for the generalized noise model.

## CONCLUSIONS

In this work it is demonstrated that the time dependence of a variety of protein associated processes can be analyzed using an inverse power law with an oscillatory component. These results suggest that a broad range of frequency modes in a protein can under certain conditions drive dynamical transitions. This work demonstrates that these conditions are not limited to specific temperature regimes or to specific processes. This provides a formal connection with critical dynamical models used to describe $1/f$ noise. Despite this connection, a specific

physical model must be developed before a direct correspondence with dynamical criticality can be made.

In this work, a chemical kinetic model is proposed that generates this power law behavior. It is based on a structural disorder model in which an average over a distribution of substates must be performed. These substates provide a dispersion in the activation energy. Again, a formal analogy with self-organized criticality exists in that averages identical to Eq. 10 are used to describe these phenomena. Self-organized criticality is characterized by nonlinear dynamics with extended spatial and temporal self-similarity. The dynamics of such systems lead to critical or metastable states. Since these states are formed from a wide variety of initial conditions, they are termed "robust attractors." We are currently exploring the formal correspondence between self-organized criticality and protein dynamics.

Protein systems may be viewed as a dynamical system in three variables: $C(t)$, $\langle C(t) \rangle$, and $\phi = kt$. These variables can be used to describe a phase space of an autonomous system. Three differential equations can be generated that couple these variables. One of the three equations (Eq. 9) is nonlinear and it is readily shown that the system is dissipative. The scaling behavior of this system establishes the temporal self-similarity. The spatial self-similarity is not as apparent. It is noted that protein backbones and surface structures are fractal and this may provide the spatial self-similarity for the system to be considered self-organized. Protein dynamics also display the robustness characteristic of self-organized criticality. Conformational transitions can be driven by a variety of perturbations and yet still lead to discrete, well defined states.

Finally, these protein dynamical models are a unique example of marginal stability in a chemical system. Marginal stability is characterized by a pure oscillatory relaxation response of a system to a perturbation. This behavior will be observed for the model in the Chemical Kinetic Model section. Instability in reaction mechanisms have traditionally been studied for cases of multistep reactions with feedback loops (for a review see reference 23). This case is unusual in that a unimolecular reaction generates marginal stability. This apparent instability is a direct result of the distribution of states. However, this marginal condition is a weak one because the inverse power law assures stability at the asymptotic, long time limit.

This research was supported in part by National Science Foundation grant DMB-9002984.

*Received for publication 2 December 1991 and in final form 24 February 1992.*

## REFERENCES

1. Dutta, P., and P. M. Horn. 1981. Low-frequency fluctuations in solids: $1/f$ noise. *Rev. Mod. Phys.* 53:487–516.
2. Weismann, M. 1988. $1/f$ noise and other slow non-exponential kinetics in condensed matter. *Rev. Mod. Phys.* 60:537–571.
3. Press, W. H. 1978. Flicker noise in astronomy and elsewhere. *Comments Astrophys.* 7:103–119.
4. Bak, P., C. Tang, and K. Wiesenfeld. 1987. Self-organized criticality: an explanation of $1/f$ noise. *Phys. Rev. Lett.* 59:381–384.
5. Bak, P., C. Tang, and K. Wiesenfeld. 1988. Self-organized criticality. *Phys. Rev. A.* 38:364–374.
6. West, B. J., and M. F. Shlesinger. 1989. On the ubiquity of $1/f$ noise. *Int. J. Mod. Phys. B.* 3:795–819.
7. Dewey, T. G., and D. B. Spencer. 1991. Are protein dynamics fractal? *Comments Mol. Cell. Biophys.* 7:155–171.
8. Shlesinger, M. F., and R. D. Hughes. 1981. Analogs of renormalization group transformations in random processes. *Physica.* 109A:597–608.
9. Millhauser, G. L. 1990. Reptation theory of ion channel gating. *Biophys. J.* 57:857–864.
10. Oswald, R. E., G. L. Millhauser, and A. A. Carter. 1991. Diffusion model of ion channel gating. *Biophys. J.* 59:1136–1142.
11. Downer, N. W., and S. W. Englander. 1977. Hydrogen exchange study of the membrane-bound rhodopsin. *J. Biol. Chem.* 252:8092–8100.
12. Knox, D. G., and A. Rosenberg. 1990. Fluctuations of protein structure as expressed in the distribution of hydrogen exchange rate constants. *Biopolymers.* 19:1049–1968.
13. Ansari, A., J. Berendzen, S. F. Bowne, H. Frauenfelder, I. E. T. Iben, T. B. Sauke, E. Shyamsunder, and R. D. Young. 1985. Protein states and protein quakes. *Proc. Natl. Acad. Sci. USA.* 82:5000–5004.
14. McManus, O. B., D. S. Weiss, C. E. Spivak, A. L. Blatz, and K. L. Magleby. 1988. Fractal models are inadequate for the kinetics of four different ion channels. *Biophys. J.* 54:859–870.
15. Bendler, J. T., and M. F. Shlesinger. 1985. Derivation of the Kohlrausch-Williams/Watts decay law from activation-energy dispersion. *Macromolecules.* 18:591–592.
16. Frauenfelder, H., F. Parak, and R. D. Young. 1988. Conformational substates in proteins. *Annu. Rev. Biophys. Biophys. Chem.* 17:451–480.
17. Frauenfelder, H., S. G. Sligar, and P. G. Wolynes. 1991. The energy landscapes and motions of proteins. *Science.* (Wash. DC). 254:1598–1603.
18. Agmon, N., and J. J. Hopfield. 1983. CO binding to heme proteins: a model for barrier height distributions and slow conformational changes. *J. Chem. Phys.* 79:2042–2053.
19. Cooper, A. 1983. Photoselection of conformational substates and the hyposochromic photoproduct of rhodopsin. *Chem. Phys. Lett.* 99:305–309.
20. Srajer, V., K. T. Schomacker, and P. M. Champion. 1986. Spectral broadening in biomolecules. *Phys. Rev. Lett.* 57:1267–1270.
21. Ormos, P., A. Ansari, D. Braunstein, B. R. Cowen, H. Frauenfelder, M. K. Hong, I. E. T. Iben, T. B. Sauke, P. J. Steinbach, and R. D. Young. 1990. Inhomogeneous broadening in spectral bands of carbonmonoxymyoglobin. *Biophys. J.* 57:191–199.
22. Steinbach, P. J., A. Ansari, J. Berendzen, D. Braunstein, K. Chu, B. R. Cowen, D. Ehrenstein, H. Frauenfelder, J. B. Johnson, D. C. Lamb, S. Luck, J. R. Mourant, G. Ulrich Nienhaus, P. Ormos, R. Philipp, A. Xie, and R. D. Young. 1991. Ligand binding to heme proteins: connection between dynamics and function. *Biochemistry.* 30:3988–4001.
23. Noyes, R. M. 1990. Mechanisms of some chemical oscillators. *J. Chem. Phys.* 94:4404–4412.